Fire Technology, 52, 1983–2003, 2016

Manufactured in The United States
DOI: 10.1007/s10694-016-0581-7

Case Study and Computational Modelling of the Impact of Fire Retardant on Fire Spread for Metal Building Insulation

Peter Senez, Adrian Milford and Keith Calder, Jensen Hughes Consulting Canada Ltd., 135-13900 Maycrest Way, Richmond, BC V6V3E2, Canada*

Received: 26 January 2015/**Accepted:** 28 February 2016

Abstract. This paper reviews a large fire loss that occurred at a seasonally operated Canadian food-processing facility. The fire occurred when the facility was not in production and started near a work area where employees had been previously unloading a trailer. The origin and cause investigation revealed different metal building insulation (MBI) products were used throughout the building on walls and ceilings. It was suspected that MBI material contributed to the rapid fire spread to otherwise empty parts of the building and that this material did not meet the relevant Building Code requirements. The facility used MBI product consisting of a polypropylene moisture barrier over fiberglass insulation. A detailed analysis of recovered MBI materials found that some of the material was flame retardant and some was not flame retardant. Additional testing of the materials was used to calibrate computational fire model inputs in order to estimate the behavior of MBI coatings by simulating fire scenarios in the full building. The intent of the analysis was to evaluate the relative propensity of the two MBI insulation products to facilitate flame spread from the area of fire origin in a comparative, qualitative framework. Test results showed that flame retardant MBI material substantially reduced fire spread compared with the non-flame retardant material. The ignition temperatures derived from cone calorimeter testing were higher (407°C compared with 226°C) and the peak heat release per unit area was lower for the flame retardant MBI coatings. The non-flame retardant MBI had a measured flame spread rating of 120, which was greater than the maximum flame spread rating of 25 permitted by the Building Code for ceiling finishes. Computational modeling correlates with non-flame retardant coated insulation (noncompliant) being present in the area where the fire originated, facilitating significant fire spread. The model predicted that the presence of non-flame retardant MBI on the ceiling facilitated flame spread across a significant distance from the area of origin within the first 300 s to 400 s, while the flame retardant MBI product yielded minimal flame spread beyond the incident area over a 20 min exposure.

Keywords: Fire retardants, Fire modelling, Flame spread, Material testing

* Correspondence should be addressed to: Adrian Milford, E-mail: amilford@sereca.com

1. Introduction

A large fire loss occurred at a seasonal Canadian food-processing and packaging facility that was not in operation at the time. Work activity within the facility on the day of the fire had been limited to the unloading of barrels from a trailer by a few employees. The fire occurred near the location where the work had taken place but after the workers had left. The fire department was notified after flames were observed from a nearby building.

The packaging and food processing structure was a single storey facility with a detached office, house and worker bunkhouse. The processing and storage structure was 10,530 m^2 in building area, and contained various types of processing and storage equipment.

The fire substantially destroyed a large northeast section of the structure including Components A, D, E, J and K with significant heat and smoke damage to Components B, C, G, L, and a portion of N. The configuration of these components is shown in Figure 1. The building had been expanded a number of times over the years preceding the fire and each letter denotes a construction permit for building modification.

2. Incident Description

2.1. Origin and Cause

The fire originated in the area circled in red in Figure 2, in the vicinity of a steel support column located at the interface of components D and K, proximal to a metal rack unit containing combustible storage items such as cardboard boxes, paint mixing equipment, paper towel rolls, and commercial cleaners. The fire likely initiated as a result of a failure of the controls for a hydraulic ramp, mounted to the support column shown in Figure 3.

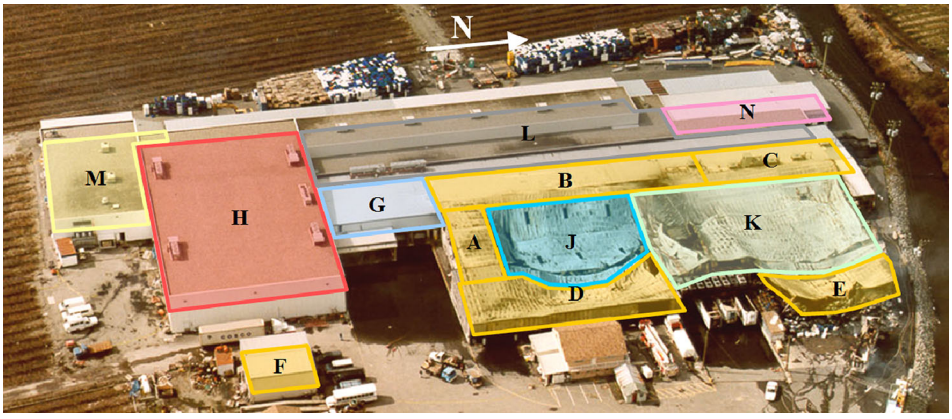

Figure 1. An aerial view of the structure with labeled building components.

Figure 2. An aerial view illustrating the area of fire origin.

Figure 3. Column A7 adjacent to the loading bay.

The fire progressed into the adjacent metal shelving unit located along the north wall of component D (Figure 4) and then extended across the roof and walls into the adjoining components. The fire rapidly spread to components A, B, C, D, E,

Figure 4. Shelving unit on north wall (*left*), and empty propane tanks for forklifts (*right*).

J, and K, with thermal damage and smoke damage extending through components L and G.

2.2. Fire Service Response

The fire was estimated to have occurred at approximately 18:15 h and the Fire Department was dispatched at 18:21 h. The first officer arrived at 18:25 h and observed flames venting from the east side of the facility and fire had spread to the majority of the structure interior. Fire suppression started at approximately 18:36 h.

The fire was under control between 22:30 h and 23:00 h, was fully contained by about 23:26 h, and was considered extinguished at 06:00 h, approximately 12 h after the fire started. The first portion of the structure collapsed approximately 1 h and 10 min after the start of the fire, and then collapsed progressively over the next 2 h, with each section ''sitting down'' as the heat caused failure of the structural steel.

2.3. Fire Spread Analysis

Even with the combustible contents of the adjacent rack storage and the proximal propane tanks (that were empty) the lack of operation and minimal building contents presented limited potential for the fire to spread laterally through the building from the area of origin. The floor area of Component D was relatively open with considerable circulation space and there was minimal commodity storage within the facility. The fuel content was therefore limited to the rack storage combustible components of the processing equipment located dominantly at the south half of Component D, and the low height storage of flattened cardboard boxes on pallets along the east side (well away from the racks).

The distances between fuel sources would allow for prolonged fire development phase prior to significant flame spread through the building (Figure 5), yet the fire department discovered the fire had spread through most of the building within minutes. The potential for fire to spread beyond the racks to the other nearby

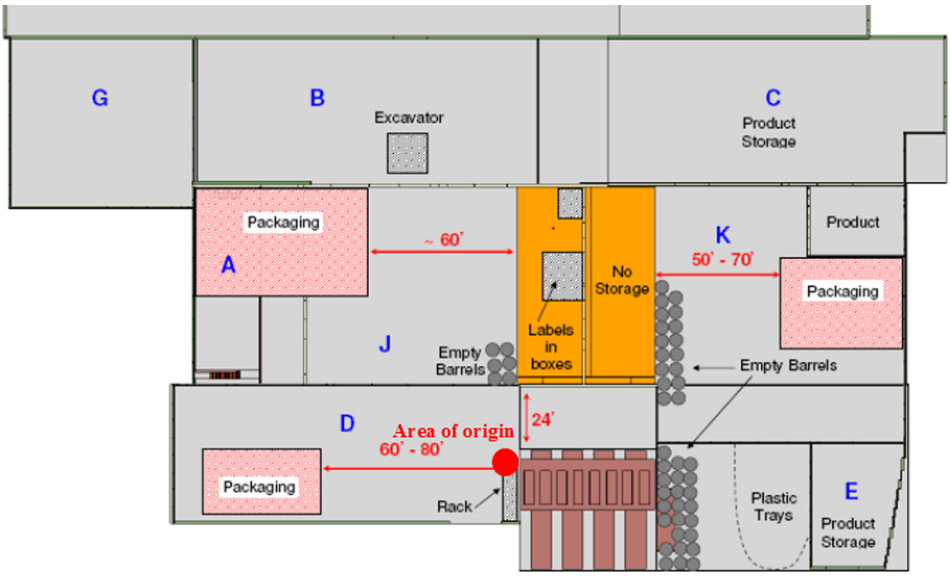

Figure 5. Fuel load distribution based on site examination.

combustible content by radiative and convective heat transfer was limited by the design of the building and floor plan. Therefore, the observed fire damage was disproportionately large for what would be expected in a building required by the Building Code to be of noncombustible construction as the requirement for flame spread ratings (maximum of 25) of the interior finish ceiling materials are intended to limit the propensity of the fire to spread in the fashion observed.

The investigation revealed the building did not conform to applicable building code requirements, which was hypothesized to have increased the potential for fire growth and spread beyond that intended by the Building Code. This resulted in significant fire development, eventually resulting in the partial collapse of the building. Key non-conformities relative to Building Code requirements included flame spread ratings of an insulation product used as the interior finish on the ceilings and walls of numerous building components, and the lack of structural fire-resistance of the unsprinklered roof assembly.

The building insulation was a composite fibreglass layer with coating of aluminum and white plastic commonly referred to as "Metal Building Insulation" or MBI. The composite coating lined the interior walls and ceilings while the fibreglass layer was sandwiched against the exterior metal cladding and metal roof. MBI insulation was observed throughout Components J, D, K, L, and N.

Two different types of building insulation were identified within Component N, neither of which was affected by the fire. One insulation type had yellow fiberglass insulation (the "Yellow Insulation"), and the other had pink fibreglass (the "Pink Insulation"). In the building sections that had collapsed due to fire, virtually all of

the insulation had been destroyed with the exception of a small section of insulation in Component D.

3. Analysis Methodology

The objective of the analysis is to evaluate the potential contribution to fire spread of two MBI products using small and large scale experimental testing and further evaluation with computational modelling, based on the following steps:

1. Determination of degree of compliance of MBI insulation product with the building code based on flame spread testing in conformance with CAN/ULC-S102.2, ''Standard Method of test for Surface Burning Characteristics of Flooring, Floor Covering, and Miscellaneous Materials and Assemblies'';
2. Chemical analysis of the surface coating of the MBI using multiple techniques to establish whether the materials contained fire retardant materials;
3. Establishing representative material properties based on small-scale cone calorimeter tests conducted in accordance with ULC-S135-04 ''Test Method for the Determination of Combustibility Parameters of Building Materials Using an Oxygen Consumption Calorimeter (Cone Calorimeter)'';
4. Validation of the material properties derived from the small scale testing using intermediate scale testing conducted in accordance with ISO 9705 ''Full Scale Room Test for Surface Products'' and a modified version of the FM Corner Test Apparatus (ANSI FM 4880-2001); and
5. A series of computer fire modelling simulations using Fire Dynamics Simulator (FDS) comparing items 3 and 4, and extrapolating the findings to the building to predict the comparative performance of the different products in a simulation of the building.

The computational analysis incorporated in this study utilizes prescribed burning-rate CFD methodology, which requires interpretation of test data from small-scale testing of the materials of interest in order to obtain representative model parameters.

The computational modelling in this study was conducted using Fire Dynamics Simulator (FDS) version 6.1.1. FDS is developed by the Building and Fire Research Laboratory at the National Institute of Standards and Technology (NIST).

The following sections of this paper detail the approach to analysis to quantifying the extent of contribution of the MBI insulation to the spread of the fire.

4. Insulation Samples

Following the fire, undamaged samples of insulation only remained in components N and L, and samples of insulation were retained for examination and further testing.

Figure 6. Metal building insulation applied to the walls and ceiling of the facility (a) Component L (b) Component N (c) Component D.

The recovered insulation was a light density fiberglass blanket. The sections were 4.87 m long by 1.22 m wide. The overall thickness was approximately 40 mm with the plastic and foil backing approximately 0.2 mm thick. Figure 6 illustrates the use of the fiberglass blanket insulation in components L, N, and D. Undamaged samples of both the Yellow and Pink MBI products in Component N were taken for further analysis.

5. CAN/ULC-S102.2 Testing

MBI insulation testing was conducted in conformance with CAN/ULC-S102.2-M88 "Standard Method of test for Surface Burning Characteristics of Flooring, Floor Covering, and Miscellaneous Materials and Assemblies" (flame spread test), the edition applicable at the time of building construction.

The flame-spread rating is an index relating to the rate of progression of a flame along a sample in a 7.6 m (25 ft) flame tunnel. A natural gas flame is applied to the front of the sample at the start and drawn along the sample by a constant draft. An observer notes the progression of the flame spread relative to time. The test apparatus and index are calibrated such that the flame spread rating for red oak is 100, and 0 for asbestos-cement board. The time and distance of flame progression are used to calculate the flame-spread rating.

The Pink MBI insulation from Component N was tested three times with a resulting flame spread rating of 120, which was greater than the maximum flame spread rating of 25 permitted by the Building Code for ceiling finishes in buildings required to be constructed of non-combustible construction.

6. Fire Retardant Content

Samples of both the Yellow and Pink insulation were evaluated by a third party using scanning electron microscopy (SEM) and energy dispersive spectroscopy (EDS). From this analysis, it was determined that the Yellow insulation vapour barrier contained bromine, chlorine, and antinomy which are elements often associated with fire retardants, while the Pink insulation did not.

Given the presence of elements associated with fire retardants in the Yellow insulation, additional testing for fire retardant content was subsequently con-

ducted on an insulation sample that was shown to be consistent with the Yellow insulation that was examined in the previous SEM and EDS testing in order to provide further understanding of the specific composition. This additional testing utilized EDS, Fourier transform infrared spectroscopy (FT-IR), and high performance liquid chromatography (HPLC). Using these methods, three polymeric film layers were identified for the coating on the fire retardant MBI sample; a layer of mineral filled polymer, a layer of flame retardant PVC with antimony trioxide, and a layer of flame retardant Polyolefin with decabromodiphenyl oxide (DecaBDE) and antimony trioxide.

7. Small Scale Testing and Material Property Derivation

Small scale testing of the MBI insulation products were conducted in conformance with ULC-S135-04 "Test Method for the Determination of Combustibility Parameters of Building Materials Using an Oxygen Consumption Calorimeter (Cone Calorimeter)". The results of these tests were used to derive material properties including ignition temperature and heat release rate (HRR) per unit area for model input.

7.1. Ignition Temperature

The derivation of ignition temperature (t_{ig}) is based upon the estimation of critical heat flux (q''_{cr}) using cone calorimeter data obtained and multiple exposure fluxes [1, 2]. For the polymer coatings of the MBI samples the material was assumed to be thermally thin. The critical heat flux for ignition was determined by determining an average time to ignition (t_{ig}) for each heat flux exposure level, correlation of $(1/t_{ig})^n$ with the cone calorimeter exposure fluxes (with n = 1 for thermally thin materials), and determination of the theoretical critical heat flux (q''_{cr}) from where linear correlation of $(1/t_{ig})^n$ with exposure heat flux intersects the abscissa (Figure 7).

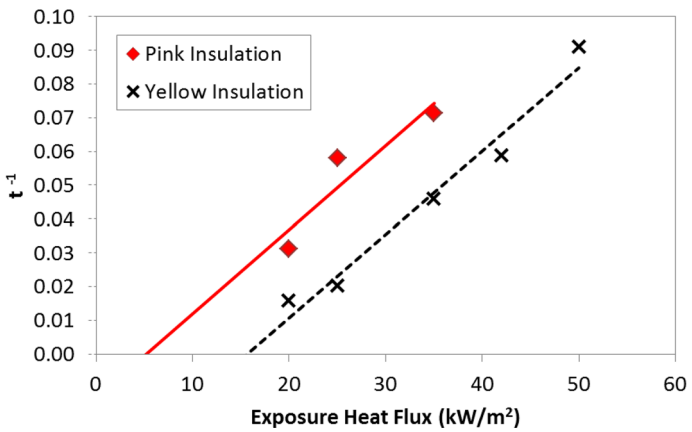

Figure 7. Determination of critical thermal heat flux.

From the theoretical critical heat flux an ignition temperature is calculated using a heat transfer analysis at the material surface using the following equation:

$$\varepsilon \cdot q''_{cr} = h_c\left(T_{ig} - T_\infty\right) + \varepsilon \cdot \sigma\left(T_{ig}^4 - T_\infty^4\right) \tag{1}$$

where $\varepsilon = 1.0$, $h_c = 10$ W/m^{2}K, $\sigma = 5.67 \times 10^{-8}$ W/m^{2}K^4, and $T_\infty = 20$°C.

The resulting estimates for ignition temperatures for the Yellow and Pink MBI insulation products were 407°C and 226°C respectively.

7.2. *Heat Release Rate per Unit Area*

The HRR per unit area was established as a function of exposure heat flux for the pink and yellow MBI insulation products, and the results are shown in Figure 8. The uncertainty of HRR measurements for Cone Calorimeter apparatuses has been previously studied by others [3–5] and based upon the data presented in these studies the relative uncertainty in the HRR measurements from the cone calorimeter testing is estimated to be approximately ±7% to 10%.

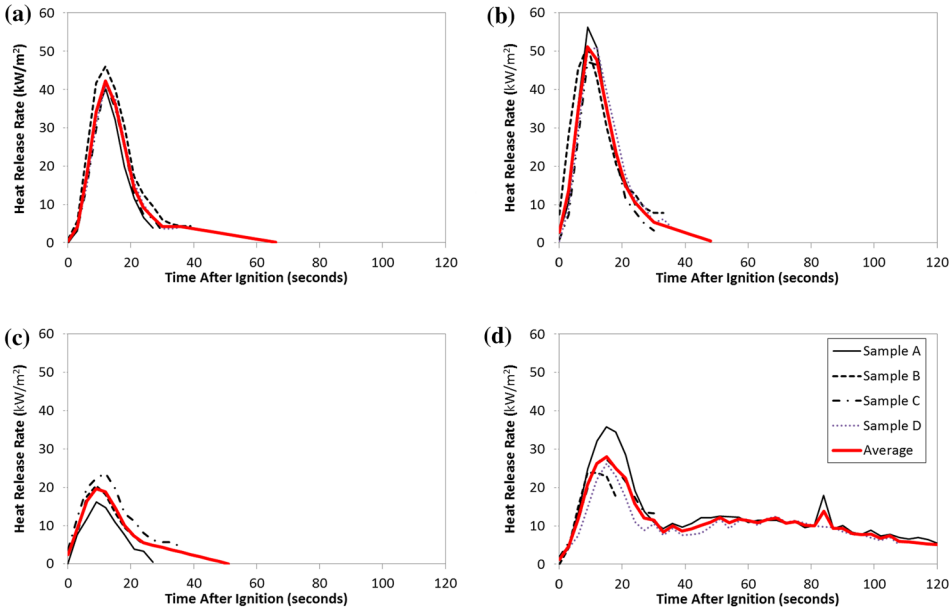

Figure 8. Cone calorimeter data for heat release rate per unit area (a) Pink insulation 25 kW/m² exposure (b) Pink insulation 35 kW/m² exposure (c) Yellow insulation 25 kW/m² exposure (d) Yellow insulation 35 kW/m² exposure.

7.3. Heat Capacity

The heat capacity per unit area of a thermally-thin material is a function of its specific heat capacity (C_p), density (ρ) and thickness (δ). Preliminary model inputs for these parameters of the pink and yellow MBI materials were derived using property estimates for polypropylene, prior to further calibration based on comparative results from the intermediate scale testing.

7.4. Use of Prescribed Burning Rates

With the prescribed burning rate methodology each material within the computational model is assigned an ignition temperature and prescribed HRR behaviour based on the derived material properties. Similar CFD methodology has been applied in the analysis of fires within residential and commercial buildings [6–8] and rapid transit vehicles [9–11].

The material-specific HRR and ignition characteristics that are derived from small scale testing serve to establish the combustion behaviour for each of the materials within the model. The model represents fire spread on the basis of a material surface reaching its specified ignition temperature, on a grid cell-by-grid cell basis. Once ignited, the material releases heat at a pre-defined time-dependent experimental burning rate ramp function that has been selected from the cone calorimeter testing at a specific incident heat flux. This is a limitation of the prescribed burning rate methodology. The burning rate of the material does not vary according to the level of incident radiation. As a result, the burning behaviour of an ignited material has the potential to be underestimated (where the actual incident heat flux is greater than the experimental heat flux), or overestimated (where the actual incident heat flux is lower than the experimental value).

Accordingly, the selection of an appropriate incident heat flux for the prescribed burning behaviour is an important assumption in the model setup in order to evaluate the predicted trends in fire development behaviour. In this analysis the intermediate scale modelling is used to evaluate appropriate values for heat flux through comparison with the test data, remaining consistent with the range of experimentally observed heat fluxes for flame spread along walls [12].

Pyrolysis modelling provides an alternative CFD methodology that allows for the effect of incident thermal radiation on the burning behaviour of materials to be accounted for in the modelling of flame spread with various materials [13]. However, pyrolysis modelling adds a significant level of complexity relative to the modelling approach when compared with the prescribed burning rate methodology, and subsequently requires additional input parameters for materials. These pyrolysis input properties require detailed derivation from experimental measurements using numerical optimization methods [14], which is beyond the scope of this paper.

8. Intermediate Scale Testing and Validation

8.1. ISO 9705 Room Fire Test

Intermediate scale testing was conducted for purposes of validating the appropriateness of the material properties derived from the small scale testing. This was

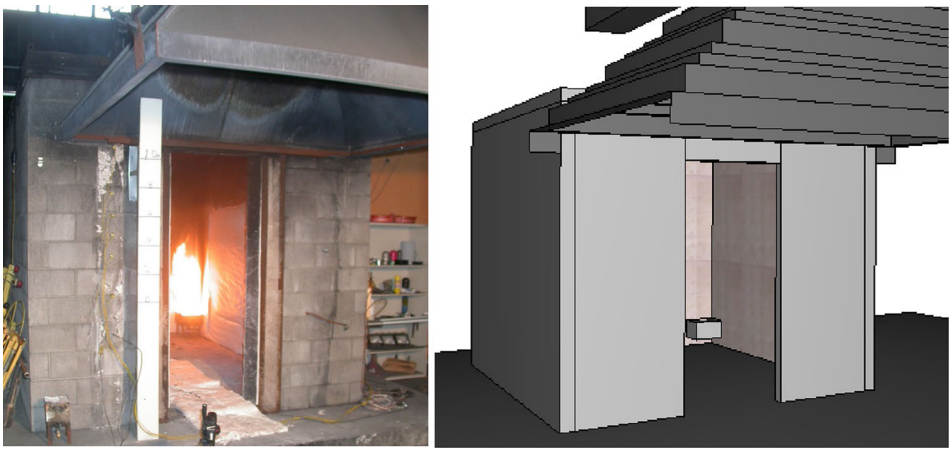

Figure 9. ISO room test apparatus (*left*) and model representation (*right*).

achieved by conducting fire tests in conformance with International Organization for Standardization ISO 9705, "Full Scale Room Test for Surface Burning Products" and comparing the results of the testing to the results of modelling of the tests using the derived material properties. Actual test apparatus and model representation are shown in Figure 9.

In this test a propane burner was located in the corner of the room opposite the door opening, and was calibrated to produce a HRR of 100 kW for the first 10 min of the test then step up to 300 kW for the following 10 min, for a test duration of 20 min. The combustion gases were collected by a hood situated above the door opening, from which the heat release and smoke production was measured.

Two tests were conducted to examine the room burning characteristics of the Pink and Yellow MBI products, with HRR and room temperatures recorded as a function of time. From the test results it was observed that the Pink insulation ignited and spread fire easily during the first stages of the test in which the burner output was 100 kW. In contrast, the Yellow insulation requires a more significant heat exposure to ignite and facilitate flame spread, which did not occur until the burner reached 300 kW.

A model of the ISO test room was constructed using the test standard specifications and programmed to have internal lining materials consistent with Pink and Yellow MBI materials with ignition temperatures and HRRs derived from the small scale testing. The insulation surfaces were specified with an insulated backing condition. A grid cell size of $0.1 \times 0.1 \times 0.075$ m^3 was implemented. For purposes of validation of the derived material properties, the HRR measured in the ISO room tests was used as a basis of comparison to the model predicted HRR.

In this instance the cone calorimeter data for Pink insulation correlates with a lower critical heat flux and ignition temperature when compared to Yellow insula-

tion. Preliminary ISO room test simulations were conducted for both insulation materials using the cone calorimeter data obtained at 25 kW/m^2 and 35 kW/m^2 exposures. Based upon the preliminary model results, the HRR behaviour was selected from the test results with 25 kW/m^2 exposure for the Pink insulation, and 35 kW/m^2 for the Yellow insulation. These values are consistent with the range of exposure values of approximately 25 kW/m^2 to 45 kW/m^2 which have been observed in experiments for flame propagation on burning walls [12, 15, 16], burning ceilings [17], and at the ceiling of modular steel sheds when subject to burning wood pallets [18]. The difference in HRR behaviour for the Pink insulation was relatively minor when comparing the 25 kW/m^2 and 35 kW/m^2; however, the heat release behaviour of the Yellow insulation exhibited a larger difference between these exposure conditions. Given the three polymer layers and fire retardant content that were identified the Yellow MBI coating, the 25 kW/m^2 exposure might correlate with limited combustion of one or more polymer layers, whereas the 35 kW/m^2 exposure appears to be sufficient to involve all of the coating layers. Selecting 25 kW/m^2 exposure data for the Pink insulation and 35 kW/m^2 exposure data for the Yellow insulation provides more onerous HRR assumptions for the Yellow insulation when evaluated in a comparative analysis.

The calibration process of the MBI model properties started with inputs for the baseline heat capacity per unit area of 0.3825 kJ/m^{2}K, using general estimates for the density and specific heat capacity of polypropylene. The preliminary model results with the baseline properties were in good agreement with the experimental HRR behaviour; however, the model inputs for $C_p\rho\delta$ were iteratively adjusted to further improve the fit of the model predictions with the experimental data, resulting in a value of 0.405 kJ/m^{2}K for the Pink insulation (C_p = 1.8 kJ/kgK, ρ = 900 kg/m^3) and 0.338 kJ/m^{2}K for the Yellow insulation (C_p = 1.5 kJ/kgK, ρ = 900 kg/m^3). Using these parameters, the resulting model predictions were in excellent agreement with the experimental data, as shown in Figures 10, 11. The calibrated input parameters for the MBI material properties were used in the subsequent modelling for the modified FM corner test and full facility scenarios.

The sensitivity of the heat release predictions to variations in C_p (evaluated over a range of 1.5 kJ/kgK to 2.1 kJ/kgK) was relatively minor, resulting in a variation of predicted peak HRR of approximately 3% for the Yellow insulation and 10% for the Pink insulation. Adjusting the value of C_p had an impact on the predicted time to peak HRR, which for the pink insulation varied from approximately 180 s (C_p = 1.5 kJ/kgK), to 190 s (C_p = 2.1 kJ/kgK), and for the yellow insulation varied from 750 s to 765 s. Variation of the material thermal conductivity from 0.1 W/mK to 0.2 W/mK was found to have negligible impact on the model predictions.

8.2. Modified FM Corner Test Apparatus (ANSI FM 4880-2001)

Insufficient MBI material remained to conduct a full FM Corner Test. However, there was sufficient Yellow insulation remaining to perform a partial test in which one wall and 4.88 m of ceiling were covered with the Yellow MBI. The test was conducted using two heptane pans (0.99 m long and 0.36 m wide) located at the

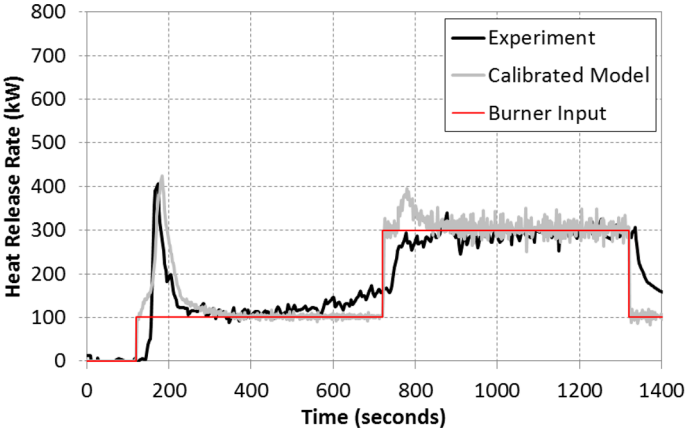

Figure 10. Heat release rate results for the pink insulation room test.

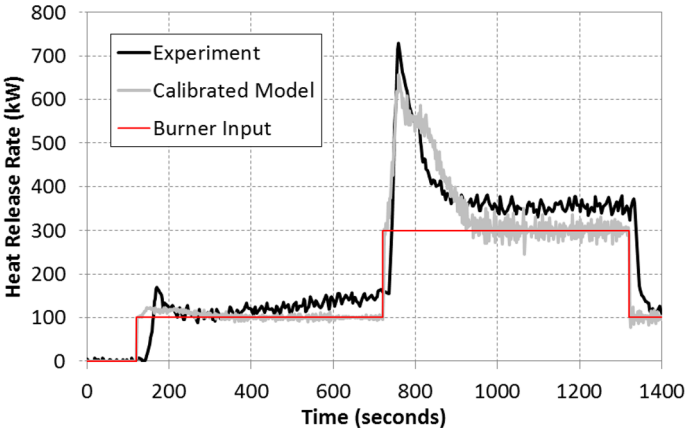

Figure 11. Heat release rate results for the yellow insulation room test.

base of the wall to evaluate the impact of significant thermal exposure over a larger wall section when compared with the ISO Room Test. In the test the insulation was ignited part way up the wall immediately above the heptane pans; however, lateral flame propagation and fire spread up to the ceiling section was not observed.

The results from a modified FM corner test apparatus were used as an additional means of validation of the material properties derived from the small scale testing and calibrated using the ISO room test. A model of the test was constructed using a grid cell size of $0.1 \times 0.1 \times 0.1$ m^3, and the model input for the heat release of the heptane pan fire was estimated using the characteristic diameter of a single pan using the following equation [19]:

$$\dot{Q}'' = m''_{\max}[1 - \exp(-k\beta D)]\Delta h_c \quad (2)$$

where $m''_{\max} = 0.101$ kg/m^{2}s, $k\beta = 1.1$ m^{-1}, and $\Delta h_c = 44{,}600$ kJ/kg.

The model results were consistent with the experimental observations of limited fire spread along the surface of the insulation, with no ignition of the ceiling panels (Figure 12). The area of insulation that was predicted to ignite in the model correlated well with the burned area from the test, as shown in Figure 13 where the burned area is localized to one portion of the exposed wall, and fire development did not continue to involve the rest of the wall and the ceiling material. The model prediction for the burned area of the wall is slightly larger than that observed in the test, which is consistent with the expected impact of assigning prescribed burning behaviour from a single exposure condition for the material. The HRR from the ignited Yellow insulation is assigned assuming a 35 kW/m^2 exposure; however, at the edges of the ignited area the actual exposure conditions would likely be lower, closer to the critical heat flux for the material. At these areas the model input for heat release would be higher than the expected heat release for exposure conditions closer to the critical heat flux, and as a result the extent of burned area would be expected to be slightly overpredicted in the model.

9. Full Building Comparative Analysis

Full building comparative analysis was conducted using the material properties that were derived from the small scale testing and validated by the mid-scale testing for input representing differing MBI types defined as wall and ceiling surfaces within a full model of the building. The purpose of the full building modelling was to predict the difference in fire spread based on the use of Pink or Yellow

Figure 12. Test footage (*left*) and fire model visualization (*right*) 2 min into the test.

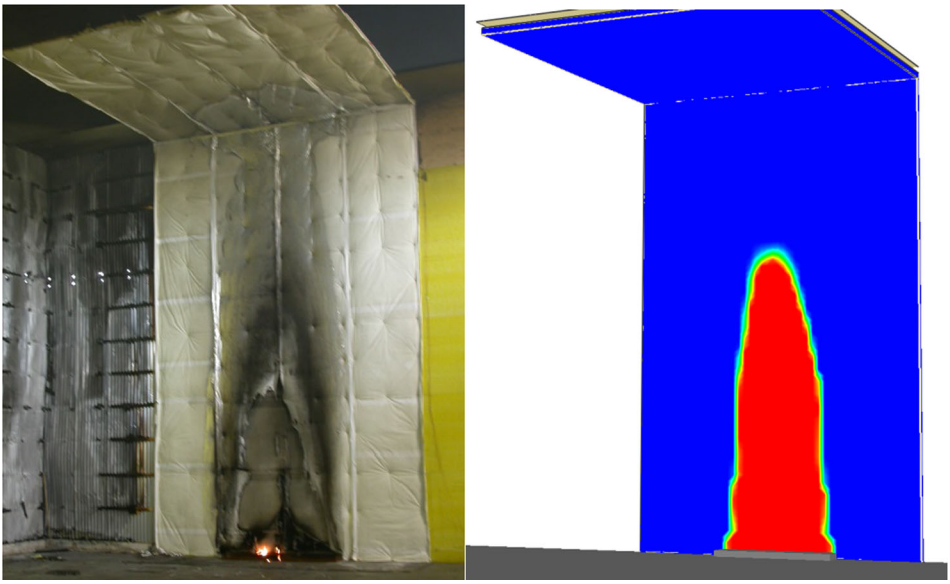

Figure 13. Extent of burned insulation from the test (*left*) compared with the model predictions of the region of insulation ignition (*right*).

insulation as wall and ceiling lining materials. The model setup and results are discussed in the following sections of this paper.

9.1. Computational Model Setup

A model representation of the building was constructed based on a combination of construction drawings and site measurements, and is shown in Figure 14.

The ignition source for the full facility simulations incorporates an initiating design fire consistent with a small pile of pallets, located at floor level and in proximity to combustible contents on rack shelving. The ignition source and combustible rack storage were not intended to represent the specific initiating source from the actual fire incident, but to provide a consistent source of sufficient size to expose the wall and ceiling lining MBI materials for the purposes of the compara-

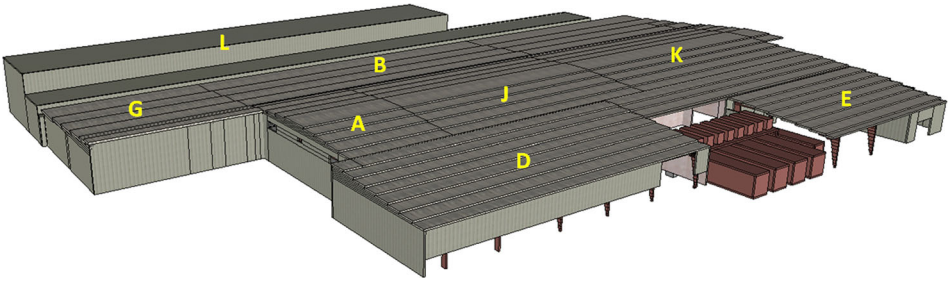

Figure 14. Model representation of the building.

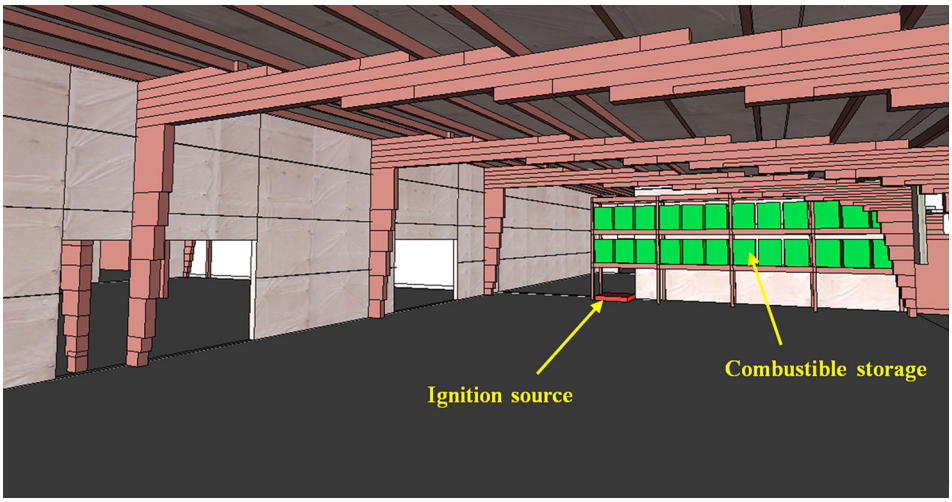

Figure 15. Model representation of the ignition source and combustible storage.

Table 1
Full Building Model Scenarios

	Building Components											
	D		J		K		A		L		B, C, & G	
Scenario	*Walls*	*Ceiling*	*Walls*	*Ceiling*	*Walls*	*Ceiling*	*Walls*	*Ceiling*	*Walls*	*Ceiling*	*Walls*	*Ceiling*
1	Pink	Pink	Pink	Pink	Pink	Pink	Yellow	Yellow	Yellow	Steel	Gypsum	Gypsum
2	Yellow	Yellow	Yellow	Yellow	Yellow	Yellow	Yellow	Yellow	Yellow	Steel	Gypsum	Gypsum
3	Pink	Yellow	Pink	Yellow	Pink	Yellow	Pink	Yellow	Pink	Steel	Gypsum	Gypsum

tive analysis. The grid cell size that were implemented were $0.1 \times 0.1 \times 0.1$ m^3 in the portion of Component D containing the initiating fire, $0.1 \times 0.1 \times 0.2$ m^3 in areas adjacent to the fire area, and $0.2 \times 0.2 \times 0.2$ m^3 throughout the remainder of the facility. The model representation of the ignition source and combustible storage within the full facility model is presented in Figure 15.

Three fire scenarios were developed to represent variations of pink and yellow wall and ceiling lining MBI materials within the building. These scenarios are summarized in Table 1. The full building scenarios were simulated for 20 min.

10. Full Building Model Results

The full building model flame spread results are shown in the following output images. The model view is from the underside of the building, looking up at the

ceiling with Pink/Yellow insulation. The black surfaces illustrate where the insulation has burned.

For Scenario 1, where the walls and ceiling of Component D are lined with Pink MBI, significant flame spread across the ceiling is predicted at the early stages of the fire, as shown at 400 s in Figure 16a. At this time flame has propagated almost the full length of Component D over a portion of the ceiling. After 1200 s a larger area of the ceiling surfaces is predicted to have ignited (Figure 16b); however, the majority of flame spread for this scenario was predicted to occur in the first 400 s.

The results of Scenario 2, where the walls and ceiling of Component D are lined with yellow MBI material, indicate very limited fire spread on the ceiling during the early stages of the fire (Figure 17a). The area in which insulation is ignited remains concentrated to the area immediately above the ignition source at the combustible rack storage. After 1200 s the extent of burned insulation is larger; however, the predicted fire spread remains concentrated to the area above the rack storage with limited spread across the width of the ceiling (Figure 17b).

The results of Scenario 3, where the ceiling of Component D is lined with Yellow MBI material and the walls are lined with Pink MBI material are almost identical to the results for Scenario 2, as shown in Figure 18. This result indicates that the wall material has limited impact on the contribution of fire spread and the material that is located on the ceiling is the most important factor relative to the predicted extent of fire spread.

The model predictions of the overall HRR for the full building scenarios are presented in Figure 19, along with a scenario with no combustible insulation

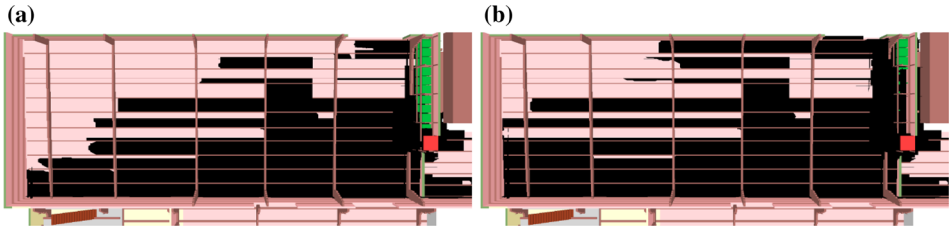

Figure 16. Model predictions of the extent of flame spread for Scenario 1. (a) 400 s (b) 1200 s.

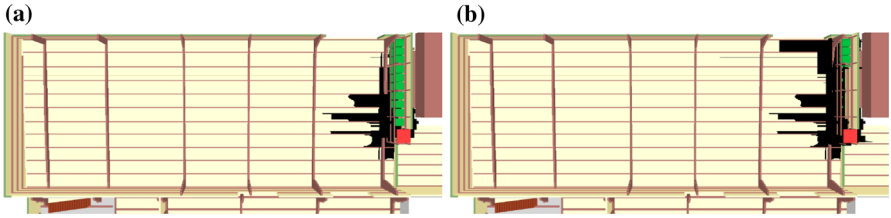

Figure 17. Model predictions of the extent of flame spread for Scenario 2. (a) 400 s (b) 1200 s.

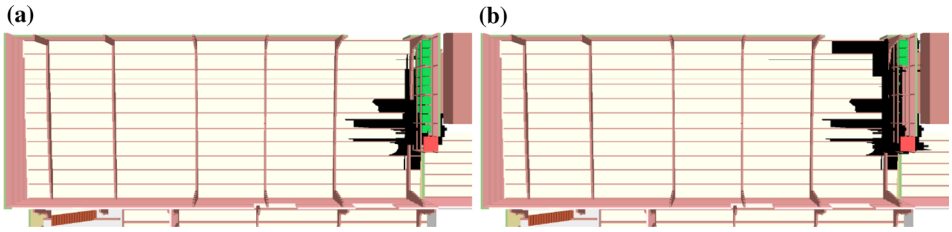

Figure 18. Model predictions of the extent of flame spread for Scenario 3 (a) 400 s (b) 1200 s.

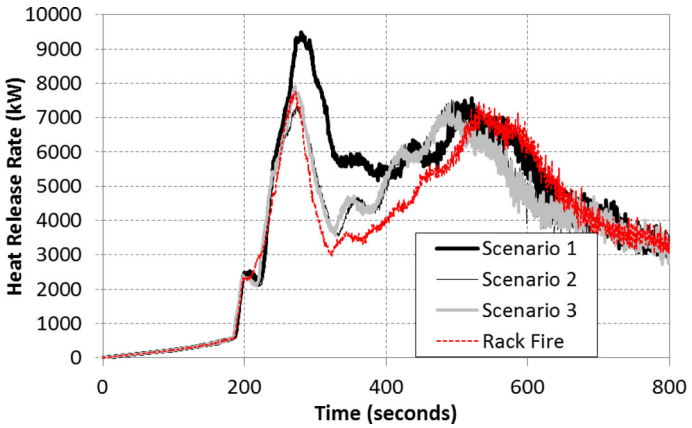

Figure 19. Model predictions of heat release rate.

which was used to characterize the HRR behaviour of the ignition source and rack contents. It should be noted that these simulations do not include the other combustible content in different areas of the facility, and are not intended to represent the full extent of fire development that was observed in the actual fire incident. The simulations include only the initiating fire and a simplified rack storage fire load to provide a representative thermal exposure to the wall and ceiling insulation in order to evaluate the potential of the MBI materials to facilitate flame spread to other areas of the building in a comparative analysis. The model results of HRR are not intended to be representative of the overall incident fire size, which would be significantly impacted by the contribution of more significant fuel load that became involved after the timescale of incipient fire spread. The following discussion of the model predictions of HRR are intended only for the purposes of comparing the predicted trends of fire development behaviour.

The combustible rack storage fire results in a HRR curve with two peaks. The first peak corresponds with the ignition and burning of the combustible content that is located immediately above the ignition source. The second peak corresponds with the subsequent ignition of the adjacent combustible materials and fire spread across the rack storage, with the greatest degree fire spread predicted across the upper levels of the rack storage.

Given the HRR behaviour of the insulation and the relatively large initiating fire representing combustible rack storage, the ignition of the insulation contributes little to the overall HRR unless the ignited area is large. For all three scenarios the early HRR behaviour is similar, as the rack storage fire provides sufficient thermal exposure to ignite both the Yellow and Pink wall insulation located immediately adjacent to the burning rack contents. The HRR curves begin to diverge near the first peak in the combustible rack storage fire, where fire spread at the Pink ceiling insulation occurs in Scenario 1, yielding a higher early HRR peak and more heat release during the first 400 s. The early ignition and rapid flame spread over a significant portion of the ceiling correlates with a higher potential for fire propagation throughout structure, when compared with Scenarios 2 and 3 in which the contribution of the insulation to the overall HRR was predominantly from the wall surfaces adjacent to the rack fire.

With Yellow insulation located on the ceiling the insulation has minimal contribution to the overall HRR until approximately 300 s. Once the insulation in the vicinity of the rack storage ignites the overall HRR increases, and the second HRR peak is achieved earlier (but with a slightly lower peak value) when compared with the rack baseline and Scenario 1. The limited flame spread on the ceiling insulation surface correlates with significantly less potential for fire spread to other areas of the building when compared with the Pink insulation ceiling finish.

11. Conclusions

This paper presents the approach developed to analyzing the growth and fire spread for a large fire in food processing facility. In the incident investigation the origin of the fire was found to be at the interface of two building components by the loading bay, and the most probable ignition source was found to be electrical. The fire was found to have spread as a result of a combustible coating on fiberglass insulation.

The objective of the comparative analysis was to compare the overall flame spread potential of two MBI products that were used within the facility. Of the two MBI products recovered from the facility, the Yellow MBI was found to limit fire spread, while the Pink product was found to readily propagate the fire. An analysis of the two materials indicated that one product contained DecaBDE flame retardant while the other product did not have fire retardants.

Testing of the MBI products was completed with a series of steps which included testing in a cone calorimeter for evaluation the material properties. The flame spread rating of the Pink insulation was found to be 120 when tested in accordance with CAN/ULC-S102.2-M88, well above the limit of 25 which is required by the applicable Building Code for ceiling finishes in buildings required to be of noncombustible construction. Burning behaviour was further evaluated using an intermediate room fire test and a full-height 25 foot wall test. Based on the cone data, an estimate was obtained for the ignition temperature and other parameters for the MBI products which were then calibrated using the FDS computer model against the output of the intermediate room tests. The testing and modelling

demonstrated the proficiency of the Yellow insulation, which was fire retardant, to resist fire spread. Conversely, the cone test, room fire test and computer modelling all indicate that the Pink Insulation, which was not fire retardant, spread the fire quickly and did not have strong fire performance characteristics.

Computational modelling of the full building using the calibrated model outputs illustrated that the insulation material on the ceiling was fundamental for the potential for flame spread. With Pink insulation on the ceiling rapid fire spread was predicted during the early stages of the fire, with significant potential for fire propagation to areas beyond the area of fire origin. Conversely, with Yellow insulation on the ceiling minimal participation of the insulation was predicted for the early stages of the fire, and once the insulation did ignite the flame spread was limited to the insulation located in the immediate vicinity of the rack storage fire.

The analysis is consistent with the presence of a MBI product with a non-fire retardant coating, resulting in a non-compliant flame spread rating along the ceiling surfaces in the area where the fire originated. The inferior products without fire retardant provided a mechanism to spread fire and smoke through the building which would not have occurred had the building complied with the applicable requirements of the building code. Had the building complied with the applicable building code requirements, instead of total destruction, the extent of fire damage would have likely remained localized to the area of fire origin.

Acknowledgments

The authors wish to acknowledge the support of the facility insurer and ICL in the development of this case study analysis.

References

1. Janssens ML, Kimble J, Murphy D (2003) Computer tools to determine material properties for fire growth modeling from cone calorimeter data. In: Proceedings of fire and materials 8th international conference, p 377–387
2. Mikkola E, Wichman I (1996) On the thermal ignition of combustible materials. Fire Mater 14:241–269
3. Enright PA, Fleischmann CM (1999) Uncertainty of heat release rate calculation of the ISO5660-1 cone calorimeter standard test method. Fire Technol 35(2):153–169
4. Brohez S (2008) Comments to the paper uncertainty of heat release rate calculation of the ISO5660-1 cone calorimeter standard test method. Fire Technol 45:381–384
5. Zhao L, Dembsey NA (2008) Measurement uncertainty analysis for calorimetry apparatuses. Fire Mater 32:1–26
6. Madrzykowski D, Vettori RL (2000) Simulation of the dynamics of the fire at 3146 cherry road NE Washington D.C., May 30, 1999, Technical Report NISTIR 6510, NIST
7. Madrzykowski D, Forney GP, Walton WD (2002) Simulation of the dynamics of a fire in a two-storey duplex—Iowa, December 22, 1999, Technical Report NISTIR 6854, NIST

8. McGrattan KB, Bouldin C, Forney GP (2005) Computer simulation of the fires in the world trade center towers, NIST NCSTAR 1-5F, NIST
9. Chiam B (2005) Numerical simulation of a metro train fire, PhD Thesis, University of Canterbury
10. Milford A, Calder K, Senez P, Coles A (2014) Computational study of tunnel ventilation effects on fire development in rapid transit vehicles. In: Proceedings of the 6th international symposium on tunnel safety and security, p 381–390
11. Milford A, Senez P, Calder K, Coles A (2014) Computational analysis of ignition source characteristics on fire development in rapid transit vehicles. In: 3rd international conference on fire in vehicles (FIVE), p 131–142
12. Babrauskas V (1993) Specimen heat fluxes for bench-scale heat release rate testing. In: Proceedings of the 6th international conference on fire science (Interflam), p 57–74
13. Lautenberger C, Wong WC, Coles A, Dembsey N, Fernandez-Pello AC (2010) Comprehensive data set for validation of fire growth models: experiments and modeling. In: Proceedings of the 12th international conference on fire science (Interflam)
14. Lautenberger C, Rein G, Fernandez-Pello C (2006) The application of a genetic algorithm to estimate material properties for fire modelling from bench-scale fire test data. Fire Saf J 41:204–214
15. Delichatsios MM, Wu O, Delichatsios MA, Lougheed GD, Crampton GP, Qian C, Ishida H, Saito K. (1994) Effect of external radiant heat flux on upward fire spread: measurements on plywood and numerical predictions. In: Proceedings of the 4th international symposium on fire safety science, p 421–432
16. Brehob EG, Kulkarni AK (1998) Experimental measurements of upward flame spread on a vertical wall with external radiation. Fire Saf J 31:181–200
17. Lattimer BY, Mealy C, Beitel J (2013) Heat fluxes and flame lengths from fires under ceilings. Fire Technol 49:269–291
18. Tinsley AT, Burdette EG, Icove DJ (2014) Structural deformations as an indicator of fire origin. J Perform Constr Facil 28:440–449
19. Gottuk DT, White DA (2008) Liquid fuel fires. The SFPE handbook of fire protection engineering, 4th edn. Society of Fire Protection Engineers, Quincy, pp 2–350